AIAA-2004-4891

A Practical Six-Degree-of-Freedom Solar Sail Dynamics Model for Optimizing Solar Sail Trajectories with Torque Constraints

Dr. Michael E. Lisano, II*

Abstract

Controlled flight of a solar sail-propelled spacecraft ("sailcraft") is a six-degree-of-freedom dynamics problem. Current state-of-the-art tools that simulate and optimize the trajectories flown by sailcraft do not treat the full kinetic (i.e. force- and torque-constrained) motion, instead treating a discrete history of commanded sail attitudes, and either neglecting the sail attitude motion over an integration timestep, or treating the attitude evolution kinematically with a spline or similar treatment. The present paper discusses an aspect of developing a next-generation sailcraft trajectory design and optimization tool at JPL, for NASA's Solar Sail Spaceflight Simulation Software (S5). The aspect discussed is an experimental approach to modeling full six-degree-of-freedom kinetic motion of a solar sail in a trajectory propagator. Early results from implementing this approach in a new trajectory propagation tool are given.

Introduction

Generally the solution for an optimal spacecraft trajectory requires that a time-history of propulsive controls (some combination the magnitude and direction of the instantaneous thrust vector, or of the velocity change vector ΔV) be computed. This is done using three-degree-of-freedom dynamics that treat the translational motion under the influence of forces acting on the spacecraft without any detailed treatment of how the spacecraft is constrained dynamically in its ability to vary in attitude from one epoch to the next. This is particularly true in state-of-the-art solar sail trajectory optimization tools, in which at best an upper limit on the solar sail attitude rate is applied as a constraint on the solar sail orientation with respect to the sun, which is the fundamental control on the solar pressure thrust vector. The present paper treats the derivation of simple, but useful, six-degree-of-freedom dynamical expressions for the translational and rotational motion of solar sails, that enables solar sail trajectory optimization to be performed with a constraint upon to the maximum allowable torque acting on a sailcraft.

One of the chief concerns at the outset of exploring this approach was the large difference in the size of propagation time steps required for accurately computing the rotation of a spacecraft, compared with that needed for computing a heliocentric spacecraft trajectory. The approach derived here is found to work well in treating solar sail rotations with attitude propagation time steps that are as large as Δt_{Trans}, with no errors in attitude accuracy. The approach also enables constraints to be applied to the torques, as opposed to the rotational rates, affecting the solar sail, which is useful in relating the trajectory optimization results to the actual sailcraft design, in that torques are relatable to the

* Group Supervisor, Navigation and Mission Design Section, Jet Propulsion Laboratory, California Institute of Technology. 4800 Oak Grove Blvd., Pasadena, CA 91109. Senior Member, AIAA.

physical system (e.g. vanes, articulated-mass systems, bias momentum wheels, thruster) that are used to control the attitude of the sailcraft.

General Six-Degree-of-Freedom Equations of Motion, and Limitations of Direct Approach

The six-degree-of-freedom state vector (that is, expressing both the translational and rotational motion) for a solar sail is formulated in a thirteen-parameter vector (Eq. 1):

$$X_{(13\times1)} = \begin{Bmatrix} \left[\bar{r}_{cg}\right]^{I} & (3\times1) \\ \left[\overset{V}{r}_{cg}\right]^{I} & (3\times1) \\ \left[\overset{V}{q}_{sc}\right]^{I}_{B} & (4\times1) \\ \left[\overset{V}{\omega}_{cg}\right]^{B} & (3\times1) \end{Bmatrix} = \begin{Bmatrix} \text{vehicle c.g. position, meters, inertial frame} \\ \text{vehicle c.g. velocity, m/sec, inertial frame} \\ \text{vehicle attitude quaternion, body frame–to–inertial frame} \\ \text{vehicle angular velocity, rad/sec, vehicle c.g.–origin body frame} \end{Bmatrix} \quad (1)$$

Here, subscript cg connotes "center of gravity"; and sc connotes "sailcraft." In the state vector, the sub-vectors $\left[\bar{r}_{cg}\right]^{I}$, $\left[\bar{v}_{cg}\right]^{I}$ and $\left[\bar{\omega}_{cg}\right]^{B}$ are all cartesian three-tuples consisting of x, y, and z components. The attitude quaternion $\left[\bar{q}_{sc}\right]^{I}_{B}$ is defined using the convention:

$$\left(\left[\bar{q}_{sc}\right]^{I}_{B}\right)^{T} = \left(\cos(\delta/2) \quad -\sin(\delta/2)\hat{i} \quad -\sin(\delta/2)\hat{j} \quad -\sin(\delta/2)\hat{k}\right)$$

in which δ is the total angle of rotation of the body frame relative to the inertial frame about the body-frame unit vector ($\hat{i}$, $\hat{j}$, $\hat{k}$).

The time six-degree-of-freedom equations of motion are found by taking the time derivative of Eq. 1, and are (Eq. 2):

$$\overset{V}{F}(X(t)) = \dot{\overset{V}{X}}_{(13\times1)} = \begin{Bmatrix} \left[\dot{\overset{V}{r}}_{cg}\right]^{I} \\ \left[\dot{\overset{V}{v}}_{cg}\right]^{I} \\ \left[\dot{\overset{V}{q}}_{cg}\right]^{I}_{B} \\ \left[\dot{\overset{V}{\omega}}_{sc}\right]^{B} \end{Bmatrix} = \begin{Bmatrix} \left[\overset{V}{v}_{cg}\right]^{I} \\ \frac{1}{M_{sc}}\left[\overset{V}{F}_{ng}\right]^{I} + \left[\overset{V}{g}_{cg}\right]^{I} \\ \frac{1}{2}\Psi_{(4\times3)}\left[\overset{V}{\omega}_{sc}\right]^{B} \\ \left\{I_{sc}\right\}^{-1}\left\{\left[\overset{V}{\tau}_{c}\right]^{B} + T^{I}_{B}\left[\overset{V}{\tau}_{env}\right]^{I} - \left[\overset{V}{\omega}_{sc}\right]^{B} \times I_{sc}\left[\overset{V}{\omega}_{sc}\right]^{B}\right\} \end{Bmatrix} \quad (2)$$

in which the time derivatives $\left[\dot{\overset{V}{v}}_{cg}\right]^{I}$ and $\left[\dot{\overset{V}{\omega}}_{sc}\right]^{B}$ are the inertial-frame acceleration of the body center of mass and the body-frame angular acceleration, and the equation variables are defined as:

M_{sc} = vehicle mass (default value = 1, never ≤ 0), scalar, kg

I_{sc} = vehicle inertia tensor (default value = $I_{3\times3}$, always full rank), 3×3, kg-m^2

$\left[\vec{F}_{ng}\right]^I$ = sum of non-gravitational forces acting at vehicle c.g. (default = $\dot{O}$), inertial frame, 3×3, kg-m/sec^2

$\left[\vec{g}_{cg}\right]^I$ = gravitational acceleration, due to N gravitating bodies, possibly with a non-spherically-distributed "primary" gravitating body, acting at vehicle c.g. (states in X), (default = $\dot{O}$), inertial frame, 3×1, m/sec^2

$\left[\vec{\tau}_c\right]^B$ = attitude control torques acting on vehicle (default = $\dot{O}$), body frame, 3×1, N-m

$\left[\vec{\tau}_{env}\right]^I$ = environment torques, such as gravity gradient torque, acting on vehicle (default = $\dot{O}$), inertial frame, 3×1, N-m

T_B^I = rotational transformation from body frame to inertial frame

$$= \begin{bmatrix} 1.0-2.0(q_2^2+q_3^2) & 2.0(q_1q_2-q_0q_3) & 2.0(q_1q_3+q_0q_2) \\ 2.0(q_1q_2+q_0q_3) & 1.0-2.0(q_1^2+q_3^2) & 2.0(q_2q_3-q_0q_1) \\ 2.0(q_1q_3-q_0q_2) & 2.0(q_2q_3+q_0q_1) & 1.0-2.0(q_1^2+q_2^2) \end{bmatrix}$$

$\left[\vec{\omega}_{sc}\right]^B$ = angular velocity of vehicle (states in X_k), body frame, 3×1, rad/sec

and the quaternion rate coefficient matrix is

$$\Psi_{(4\times3)} = \begin{bmatrix} -q_1 & -q_2 & -q_3 \\ q_0 & -q_3 & q_2 \\ q_3 & q_0 & -q_1 \\ -q_2 & q_1 & q_0 \end{bmatrix}$$

These equations of motion are general for a rotating or non-rotating rigid body influenced by gravitational and non-gravitational effects. The only non-gravitational force treated here is the solar radiation pressure force ($\vec{F}_{srp}$), which is computed with the standard optical model[1, 2] as in Eq. 3:

$$\left[\vec{F}_{ng}\right]^I = \left[\vec{F}_{srp}\right]^I = P(r_{sc/sun}) \times A_{sail}\left(-\{a_1\cos^2(\alpha)+a_2\cos(\alpha)\}\hat{n}+\{a_3\sin(\alpha)\cos(\alpha)\}\hat{t}\right) \quad (3)$$

in which:

$r_{sc/sun}$ = distance of the sailcraft from to the center of the sun (km)
$P(r_{sc/sun})$ = solar radiation pressure as a function of sun/sailcraft distance (N/m^2)
A_{sail} = total light-reflecting area of the sail (m^2)
$a_1 = 1 + \rho s$
$a_2 = B_f(1 - s)\rho + (1 - \rho)(\varepsilon_f B_f - \varepsilon_b B_b) / (\varepsilon_f + \varepsilon_b)$
$a_3 = 1 - \rho s$
ρ = sail material reflectivity (dimensionless, ranges from 0 to 1)
s = fraction of reflectivity that is specular (dimensionless, ranges from 0 to 1)
ε_f = thermal emissivity of sail front side (sunward) material (dimensionless)

ε_b = thermal emissivity of sail back side (anti-sunward) material (dimensionless)
B_f = fraction of sail front-side reflectance that is non-Lambertian (0 – 1)
B_b = fraction of sail back-side reflectance that is non-Lambertian (0 – 1)
$\hat{n}$ = unit normal vector, perpendicular to the sailcraft reflecting area
$\hat{r}_0$ = unit sun-direction vector, from center of the sun to the sailcraft
α = "cone angle" = acos(- $\hat{n} \cdot \hat{r}_0$)

$$\hat{t} = \text{unit transverse vector, } = -\frac{\hat{n} \times (\hat{n} \times \hat{r}_0)}{\left\| \hat{n} \times (\hat{n} \times \hat{r}_0) \right\|}$$

Eqs. 2 possess the desirable aspect that the coupled attitude motion and translational motion have an explicit, linear dependency on the control torque $[{}^{V}\tau_c]^{B}$ acting on the sailcraft. Early in this study, an attempt was made to leverage this mathematical feature so that the control torque history (as opposed to a history of sail inertial attitudes, which represents state-of-the-art practice - c.f. refs. 2, 3, 4, 5) would be computed to minimize time-of-flight. However, two problems were encountered in designing an optimization tool that models the full six-degree-of-freedom coupled rigid-body dynamics, and treats $[{}^{V}\tau_c]^{B}$ vs. time as the control. First, it was difficult to assign an initial guess for the time history of torques, to start the optimization process; in other words, it is more straightforward to envision and supply a physically-meaningful sequence of attitudes (e.g. in terms of sail normal vector cone and clock angles) than a sequence of torques. This problem is one of ease-of-use by a trajectory designer, and while it is not necessarily insurmountable, it calls for a user interface design activity that could be at least as challenging as the development of the optimization algorithms themselves.

Second, a numerical issue arises with the propagation in time of Eqs. 2. It has been experimentally determined that the translational equations of motion can be propagated with acceptable accuracy for trajectory design problems involving heliocentric flight of solar sails using an integration step size Δt_{Trans} on the order of 86400 sidereal sec, or even larger. For example, numerically integrating a heliocentric solar sail trajectory using Sperling-Burdet elements (c.f. Bond and Allman[6]) using $7^{th}/8^{th}$-order Runge-Kutta with a 1-day time step results in trajectory errors on the order of . However, for accurate propagation of the rotational equations of motion, it is found – again, by experimentation – that an integration time step Δt_{Rot} typically on the order of 1 second or smaller is required to maintain a small attitude error (nominally < 0.1 deg error in one day). This property in the equations of motion is referred to as *stiffness*[7]. Propagating Eqs. 2 with a 1-second time step would result in runtimes about four orders of magnitude slower than a three-degree-of-freedom trajectory propagation tool. Moreover, the accuracy of the resulting translational trajectory would be affected by an accumulation of truncation errors over many small time steps.

As a result of these issues, an approach was sought that would allow for propagation of the solar sail trajectory with large time steps, while accurately modeling the rotational motion of the sailcraft. An analytic expression for the solar sail rotation, subject of the remainder of this paper, is key to this alternative approach to modeling this six-degree-of-freedom, torque-constrained dynamical system.

Analytic Expression for Solar Sail Rotation under Constant Torque

Consider the rotational equations of motion, extracted from Eq. (2) and neglecting environmental torques (Eq. 4):

$$\left[\dot{\vec{\omega}}_{sc}\right]^B = \{I_{sc}\}^{-1}\left\{\left[\vec{\tau}_c\right]^B - \left[\vec{\omega}_{sc}\right]^B \times I_{sc}\left[\vec{\omega}_{sc}\right]^B\right\} \qquad (4)$$

Let us assume that the solar sail has constant spin rate $\omega_z = \omega_{z0}$; that is, control torques are to be applied only about the sailcraft body x and y axes. Moreover, let us assume that the sailcraft is axisymmetric about the z axis, so that the sail inertial tensor is (Eq. 5):

$$I_{sailcraft} = \begin{bmatrix} I + m_{PL}b_{PL}^2 & 0 & 0 \\ 0 & I + m_{PL}b_{PL}^2 & 0 \\ 0 & 0 & 2I \end{bmatrix} \qquad (5)$$

where:
I = moment of inertia of sail membrane and its structural supports (kg m^2)
m_{PL} = payload mass (kg), supported at end of a boom along the + sailcraft z axis
b_{PL} = payload boom length (m)

With the above assumptions, and dropping the $[.]^B$ notation, Eq. 4 becomes (Eqs. 6):

$$\begin{aligned} \dot{\omega}_x &= \frac{\tau_x}{(I + m_{PL}b_{PL}^2)} - \lambda\omega_z\omega_y \\ \dot{\omega}_y &= \frac{\tau_y}{(I + m_{PL}b_{PL}^2)} + \lambda\omega_z\omega_x \qquad (6) \\ \dot{\omega}_z &= \frac{\tau_z}{2I} = 0 \end{aligned}$$

in which $\lambda = (I - m_{PL}b_{PL}^2)/(I + m_{PL}b_{PL}^2)$.

Next, the variation-of-parameters technique was used to find a solution for Eqs. 6, given the added assumption that the control torques tx and ty are constant. This results in expressions for the body-frame rotation rates under constant x- and y-axis torques (Eqs. 7):

$$\omega_x(t) = \left\{\omega_{x0} + \left[\frac{\tau_y}{I\lambda\omega_{z0}}\right]\right\}\cos[\lambda\omega_{z0}(t - t_0)] - \left\{\omega_{y0} - \left[\frac{\tau_x}{I\lambda\omega_{z0}}\right]\right\}\sin[\lambda\omega_{z0}(t - t_0)] - \left[\frac{\tau_y}{I\lambda\omega_{z0}}\right]$$

$$\omega_y(t) = \left\{\omega_{y0} - \left[\frac{\tau_x}{I\lambda\omega_{z0}}\right]\right\}\cos[\lambda\omega_{z0}(t - t_0)] + \left\{\omega_{x0} + \left[\frac{\tau_y}{I\lambda\omega_{z0}}\right]\right\}\sin[\lambda\omega_{z0}(t - t_0)] + \left[\frac{\tau_x}{I\lambda\omega_{z0}}\right] \quad (7)$$

$$\omega_z(t) = \text{constant} = \omega_{z0}$$

Note that the expressions in Eqs. 7 are finite and analytic for all finite values of ω_z, including $\omega_z = 0$. This is proven in a straightforward fashion by expanding the $\sin[\lambda\omega_z(t-t_0)]$ and $\cos[\lambda\omega_z(t-t_0)]$ terms into Taylor series.

Define the body-frame angular displacement variables $\Delta\theta_x$, $\Delta\theta_y$, $\Delta\theta_z$ as (Eq. 8):

$$\Delta\theta_x \equiv \int_{t_0}^{t} \omega_x(t)\, dt$$

$$\Delta\theta_y \equiv \int_{t_0}^{t} \omega_y(t)\, dt \quad (8)$$

$$\Delta\theta_z \equiv \int_{t_0}^{t} \omega_z(t)\, dt$$

For the constant-x-and-y-torque case, we substitute Eqs. (7) into Eqs. (8) and solve. The resulting body-frame angular displacements are (Eq. 9):

$$\Delta\theta_x(t) = \left\{\frac{\omega_{x0}}{\lambda\omega_{z0}} + \left[\frac{\tau_y}{I(\lambda\omega_{z0})^2}\right]\right\}\sin[\lambda\omega_{z0}(t - t_0)] +$$
$$\left\{\frac{\omega_{y0}}{\lambda\omega_{z0}} - \left[\frac{\tau_x}{I(\lambda\omega_{z0})^2}\right]\right\}\{\cos[\lambda\omega_{z0}(t - t_0)] - 1\} - \left[\frac{\tau_y}{I\lambda\omega_{z0}}\right](t - t_0)$$

$$\Delta\theta_y(t) = \left\{\frac{\omega_{y0}}{\lambda\omega_{z0}} - \left[\frac{\tau_x}{I(\lambda\omega_{z0})^2}\right]\right\}\sin[\lambda\omega_{z0}(t - t_0)] + \quad (9)$$
$$\left\{\frac{\omega_{x0}}{\lambda\omega_{z0}} + \left[\frac{\tau_y}{I(\lambda\omega_{z0})^2}\right]\right\}\{\cos[\lambda\omega_{z0}(t - t_0)] - 1\} + \left[\frac{\tau_x}{I\lambda\omega_{z0}}\right](t - t_0)$$

$$\Delta\theta_z(t) = \omega_{z0}(t - t_0)$$

As with Eqs. 7, the expressions in Eqs. 9 are finite and analytic for all finite values of ω_z, including $\omega_z = 0$. Eqs. 7 and 9 are a complete analytical solution for the rotational motion of an axisymmetric rigid-body solar sail affected by constant x- and y-axis torques. Contrasted with a numerical integration (using order-1-sec time steps) of the rotational equations in Eqs. 2, these analytical expressions can be evaluated over arbitrarily large time steps, and produce results that are not degraded by truncation roundoff error. Thus, if a time history of x- and y-axis control torques is provided, along with initial position, velocity, attitude and attitude rate information, the translational and rotational motion of the sail can be propagated with "large" time steps Δt_{Trans}, by evaluating Eqs. 7 and 9 in the translational equations of motion.

However, as discussed above, providing the time history of torques as an input is still problematic. Hence a method was sought for targeting the x- and y-axis torques, given a desired sailcraft attitude history (consistent with state-of-the-art sailcraft trajectory design practice).

Attitude Targeting Algorithm for Determination of Torques

Now if we apply a constant torque over time increment dt, having body-frame x- and y-components τ_x and τ_y, to a solar sail having a constant spin rate ω_z and initial body rates ω_{x0} and ω_{y0}, the resulting body-frame angular displacement components are given by Eqs. 9 above, and the resulting body rates are given by Eqs. 7 above. Define Δt as $(t - t_0)$. As $\Delta\theta_z(t)$ is independent of τ_x, τ_y, ω_{x0} and ω_{y0}, we separate the z-component out from these equations, leaving expressions for $\Delta\theta_x(t_0 + \Delta t)$, $\Delta\theta_y(t_0 + \Delta t)$, $\omega_x(t_0 + \Delta t)$ and $\omega_y(t_0 + \Delta t)$ that are linear functions of ω_{x0}, ω_{y0}, τ_x and τ_y. We can also rearrange these linear expressions to solve for $\Delta\theta_x(t_0 + \Delta t)$, $\Delta\theta_y(t_0 + \Delta t)$, ω_{x0}, and ω_{y0}, as linear functions of $\omega_x(t_0 + \Delta t)$, $\omega_y(t_0 + \Delta t)$, τ_x and τ_y (Eqs. 10):

$$\begin{Bmatrix} \Delta\theta_x(t_0+\Delta t) \\ \Delta\theta_y(t_0+\Delta t) \\ \omega_{x0} \\ \omega_{y0} \end{Bmatrix} = K_{4x4}(I,\ \lambda,\ \omega_{z0},\ \Delta t) \begin{Bmatrix} \omega_x(t_0+\Delta t) \\ \omega_y(t_0+\Delta t) \\ \tau_x \\ \tau_y \end{Bmatrix} \qquad (10)$$

in which the components of (4 x 4) matrix K are:

$k_{11} = \{\sin(\lambda\omega_z\Delta t)\}/(\lambda\omega_z)$
$k_{12} = \{\cos(\lambda\omega_z\Delta t) + 1\}/(\lambda\omega_z)$
$k_{13} = \{\cos(\lambda\omega_z\Delta t) - 2\}/(I\,\lambda\omega_z)$
$k_{14} = \{\sin(\lambda\omega_z\Delta t) - \Delta t\}/(I\,\lambda\omega_z)$
$k_{21} = -\{\cos(\lambda\omega_z\Delta t) + 1\}/(\lambda\omega_z)$
$k_{22} = \{\sin(\lambda\omega_z\Delta t)\}/(\lambda\omega_z)$
$k_{23} = -\{\sin(\lambda\omega_z\Delta t) - \Delta t\}/(I\,\lambda\omega_z)$
$k_{24} = \{\cos(\lambda\omega_z\Delta t) - 2\}/(I\,\lambda\omega_z)$
$k_{31} = \cos(\lambda\omega_z\Delta t)$
$k_{32} = \sin(\lambda\omega_z\Delta t)$

$k_{33} = -\{\sin(\lambda\omega_z\Delta t)\}/(I\,\lambda\omega_z)$
$k_{34} = \{\cos(\lambda\omega_z\Delta t) - 1\}/(I\,\lambda\omega_z)$
$k_{41} = -\sin(\lambda\omega_z\Delta t)$
$k_{42} = \cos(\lambda\omega_z\Delta t)$
$k_{43} = -\{\cos(\lambda\omega_z\Delta t) - 1\}/(I\,\lambda\omega_z)$
$k_{44} = -\{\sin(\lambda\omega_z\Delta t)\}/(I\,\lambda\omega_z)$

Given the desired body-frame angular displacements and the initial-time body rates $\{\Delta\theta_x(t + \Delta t),\ \Delta\theta_y(t + \Delta t),\ \omega_{x0}, \text{ and } \omega_{y0}\}$, we can solve for the final-time body rates and the required constant x- and y- torques $\{\omega_x(t + \Delta t),\ \omega_y(t + \Delta t),\ \tau_x, \text{ and } \tau_y\}$ needed to attain the angular displacements. This is done as shown in (Eq. 11):

$$\begin{Bmatrix} \omega_x(t_0 + \Delta t) \\ \omega_y(t_0 + \Delta t) \\ \tau_x \\ \tau_y \end{Bmatrix} = L_{4x4}(I,\ \lambda,\ \omega_{z0},\ \Delta t) \begin{Bmatrix} \Delta\theta_x(t_0 + \Delta t) \\ \Delta\theta_y(t_0 + \Delta t) \\ \omega_{x0} \\ \omega_{y0} \end{Bmatrix} \qquad (11)$$

in which L is the pseudo-inverse of K, i.e. $L = (K^T K)^{-1} K^T$.

Eqs. 11 are the basis of a solar torque targeting algorithm (for an axisymmetric, rigid-body, constant-spin-rate solar sail having a payload mass concentrated at the end of a boom on the body z axis), which takes a commanded angular change (expressed in terms of $\Delta\theta_x$, $\Delta\theta_y$, and returns the needed torques τ_x, τ_y (constant over the time interval Δt).

In order to implement torque targeting in a trajectory propagator, one must determine the desired body-frame angular displacements $\Delta\theta_x$, $\Delta\theta_y$ from time t_0 till time t. As noted above, typically a solar sail control is provided in terms of a time sequence of cone angle, clock angle pairs (α, β). Hence, an approach was needed to relate a desired change in cone and clock angle ($\Delta\alpha$, $\Delta\beta$) to the body-frame angular displacements. See Fig. 1 for an illustration of the difference between these angle changes.

An approach to relating ($\Delta\theta_x$, $\Delta\theta_y$) to ($\Delta\alpha$, $\Delta\beta$) is based on noting the relationship between the sail normal vector in both the body and inertial reference frames at t_0 and time t. That is, the inertial-frame sail normal vector at time t, $\hat{n}_I(t)$, is related to the initial-time inertial-frame sail normal vector $\hat{n}_I(t_0)$, by (Eq. 12):

$$\hat{n}_I(t) = T_{3,I}(\Delta\beta)\ T_{1,I}(\Delta\alpha)\ \hat{n}_I(t_0) \qquad (12)$$

in which $T_{1,I}(\Delta\alpha)$ is a 3x3 orthogonal transformation matrix expressing the rotation $\Delta\alpha$ about the inertial x axis and $T_{3,I}(\Delta\beta)$ is for rotation $\Delta\beta$ about the inertial z axis.

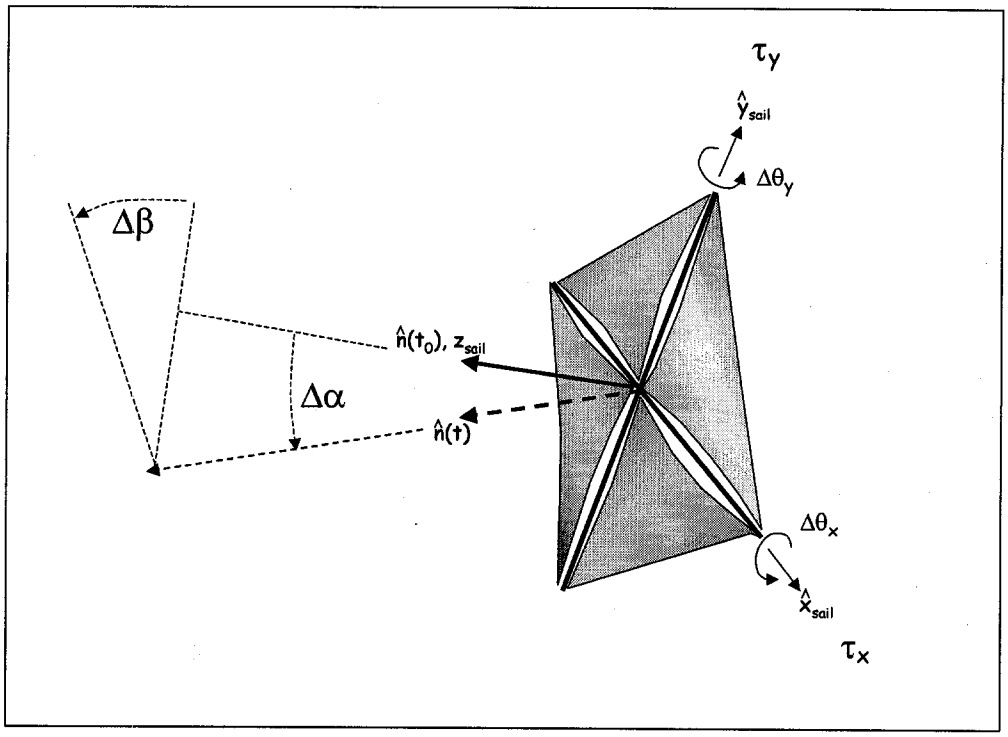

Figure 1. Solar Sail Body-Frame Angular Displacements $\Delta\theta_x$, $\Delta\theta_y$, and Commanded Sail Cone and Clock Angle Changes $\Delta\alpha$, $\Delta\beta$

Now relating $\hat{n}_I(t)$ to the body-frame initial-time normal vector is $\hat{n}(t_0)$ requires taking into account the orthogonal transformation from the body frame to the inertial frame at time t_0 (Eq. 13):

$$\hat{n}_I(t) = T_{3,I}(\Delta\beta)\, T_{1,I}(\Delta\alpha) T_B^I(t_0)\, \hat{n}(t_0) \qquad (13)$$

Next, we can relate the body-frame normal vector at time t, $\hat{n}(t)$, to $\hat{n}(t_0)$ by taking into account the orthogonal transformation from the inertial frame to the body frame at time t (Eq. 14):

$$\hat{n}(t) = T_I^B(t)\, T_{3,I}(\Delta\beta)\, T_{1,I}(\Delta\alpha) T_B^I(t_0)\, \hat{n}(t_0) \qquad (14)$$

We can also relate $\hat{n}(t)$ to $\hat{n}(t_0)$ by applying a sequence of body-frame angular displacements about the x, then y (or y, then x) body axes, as in Eq. 15:

$$\hat{n}(t) = T_{2,B}(\Delta\theta_y)\, T_{1,B}(\Delta\theta_x)\, \hat{n}(t_0) \qquad (15)$$

In Eq. 15, $T_{1,B}$ and $T_{2,B}$ are orthogonal transformations about the body-frame x and y axes, respectively. Now the coefficients of $\hat{n}(t_0)$ in Eq. 14 and Eq. 15 can be equated to one another (Eq. 16):

$$T_{xy} \equiv T_{2,B}(\Delta\theta_y)\, T_{1,B}(\Delta\theta_x) = T_I^B(t)\, T_{3,I}(\Delta\beta)\, T_{1,I}(\Delta\alpha) T_B^I(t_0) \qquad (16)$$

Finally, terms a_{ij} from 3x3 orthogonal matrix T_{xy} are solved for $\Delta\theta_x$ and $\Delta\theta_y$, i.e.:

$$\Delta\theta_x = \sin^{-1}(-a_{23})$$
$$\Delta\theta_y = \tan^{-1}\left(\frac{a_{13}}{a_{33}}\right) \qquad (17)$$

Note that the right-hand-side of Eq. 16 contains body-to-inertial/inertial-to-body transformation matrices at two times. This implies that, although we are not requiring the attitude quaternion q or the body rate vector ω to be in the state vector, we must book-keep the sailcraft inertial attitude as a function of time in the propagation software, in order to allow evaluation of $T_I^B(t)$ and $T_B^I(t_0)$. Also, solving Eq. 16 requires an iterative technique, because the inertial-to-body transformation at time t is a function of the attitude at time t, which is, in turn, a function of the torques that we are solving for in the targeting equations.

This approach for finding $\Delta\theta_x$ and $\Delta\theta_y$ given some commanded change in cone and clock angle ($\Delta\alpha$, $\Delta\beta$), is used, in conjunction with the torque-targeting equations (Eqs. 12), and the constant-torque rotational equations of motion (Eqs. 7 and 9), to model the inertial rotation of the solar sail, under the effect of torques, in a trajectory propagator.

Implementing Torque-Targeted Attitude Modeling in a Trajectory Propagator

The approach discussed above, for targeting torques based on input cone and clock angles, then modeling the rotational motion of a rigid-body sailcraft based on those torques, was implemented in the sailcraft trajectory propagation routine being developed for NASA's Solar Sail Spaceflight Simulation Software (S5)[8]. The translational equations of motion, which are evaluated multiple times in a Runge-Kutta numerical integrator at each propagation time step, were modified accept as input a sailcraft attitude that varied over each time step. In this initial implementation, only a non-spinning sailcraft has been treated; the control torques are selected to bring first the sail X axis, then the sail Y axis, from zero body rate, to a maximum body rate at mid-attitude-maneuver, then back to zero body rate at the targeted new attitude. Stated differently, there are four daily torque segments, with the X torque applied in the positive, then negative, sense, and then the Y torque applied in the positive, then negative, sense. Prescribing zero body rates at the time step boundaries was an arbitrary choice, but is a simple method for keeping the body rates bounded over the trajectory leg.

A note on the magnitude of the torques: the torques are targeted to reach the final state no earlier than the final time, so that there is no period during the time step (typically 86400 seconds) that the sailcraft is un-torqued and "coasting" in rotational motion. This choice results in keeping the torque levels over each segment minimal (and hence, hopefully, achievable by whatever attitude control method – e.g. vanes, differential motion of center-of-mass to center of pressure, wheels or tip thrusters – is chosen for the vehicle.

The "6DOF-modified" translational propagator was tested with the initial conditions and optimal control discrete time history that had been generated by C. W. Yen of JPL using the legacy SAIL solar sail trajectory optimizer, for the Geostorm solar sail mission[9]. See Fig. 2 for a plot of three versions of the trajectory, displayed in the synodic Earth/Sun frame, with axes centered at Earth. The sailcraft is assumed to have a total mass of 297 kg, with a 10,000 m^2 square sail reflective surface; gravity effects of the Earth, Moon, Sun and Venus are all modeled. Sail attitude is constrained to have a cone angle not greater than 45 degrees.

These trajectory versions were all created with the 6DOF-modified propagator, in three different modes. The first trajectory, which terminates near the white triangle in the figure, was computed with constant attitude over each 1-day time step. It arrives within approximately 50,000 km RSS of the location predicted by SAIL. The second trajectory, which terminates near the black triangle in the figure, was computed using a continuously-varying attitude based on targeted torques. It arrives approximately 350,000 km from the location predicted by SAIL. The third trajectory, which is nearly overlaid on the first trajectory and also terminates near the white triangle in the figure, was computed with continuously-varying attitude based on targeted torques, but was modified so that the sailcraft was 1 kg heavier (i.e. 298 kg). It arrives approximately 30,000 km from the location predicted by SAIL.

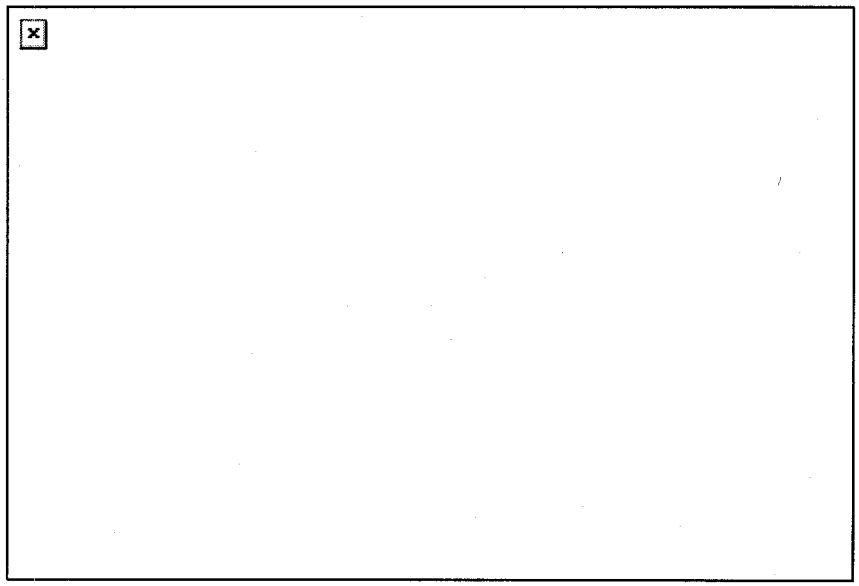

Figure 2: 286-day Geostorm Sailcraft Transfer Trajectory from Earth-Sun L1 Point to Sub-L1 Equilibrium Point on Earth-Sun Line

The optimal control history from the SAIL software was provided as a time series of sail cone and clock angles (see Fig. 3, left side, for the control history) with a typical time step of 1 day. The 6DOF-modified propagator varied the attitude continuously over each time step – the difference between the attitude that was propagated with targeted torques in the integrator, and the commanded attitude (in terms of cone and clock angles) is shown in Fig. 3, on the right side. The attitude is seen to generally match with very high

accuracy – however, it is also noted that the maximum difference in attitude is seen to be a "spike" of about half a degree, around mid-trajectory (when the largest commanded change in attitude for the trajectory occurs).

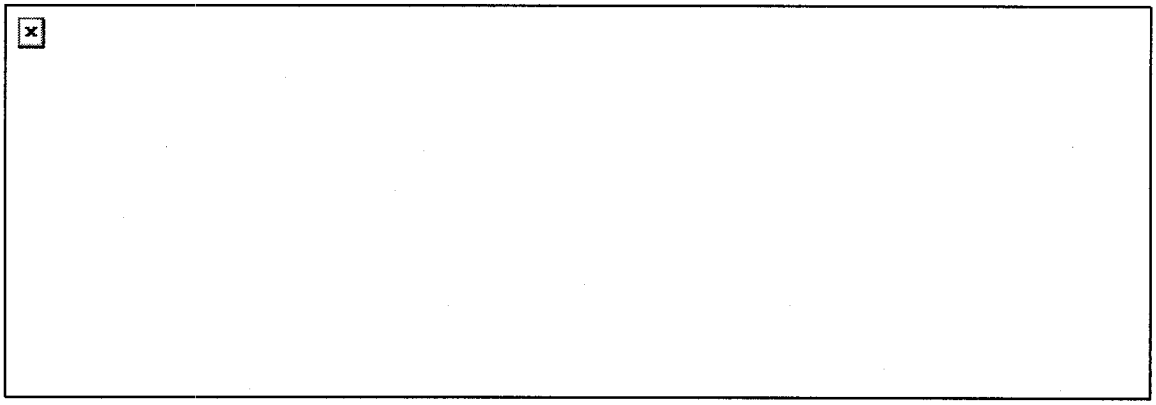

Figure 3: (left) Commanded Sailcraft Cone and Clock Angle History for Geostorm Mission[9]; (right) difference between propagated Cone and Clock Angles (using torque targeting technique) and Commanded Values

Finally, the "targeted torques" approach to modeling the attitude yields outputs from the trajectory propagator which can be of use in designing a sailcraft mission. In particular, a preliminary control torque history profile can be generated (see Fig. 4 for the Geostorm torque history produced in this fashion), as well as a prediction of the peak body rates over each interval between commanded attitudes (see Fig. 5 for the peak body rate history for Geostorm).

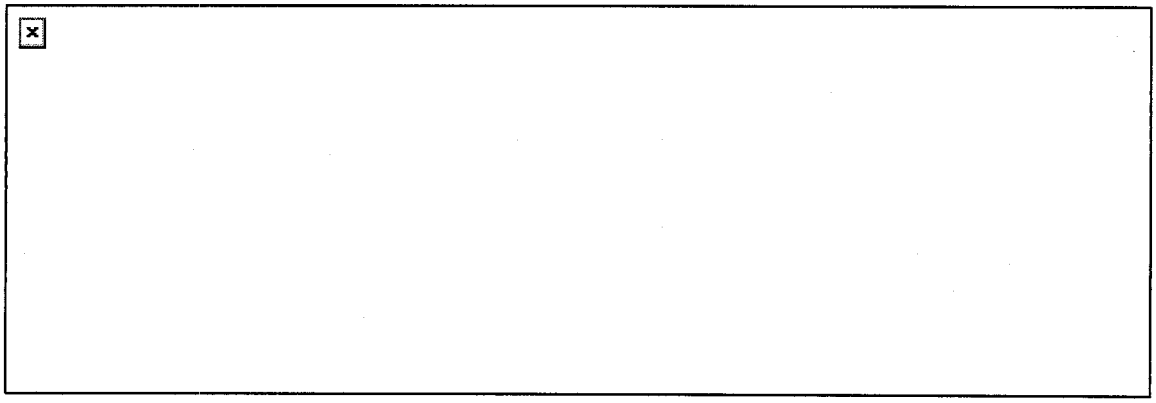

Figure 4: (left) Geostorm Sailcraft Torque History (assuming X, then Y axis torque sequence) for entire L1-to-sub-L1 transfer, based on commanded cone and clock angles; (right) Geostorm Torque History (Five Days centered at mid-trajectory "spike" in torque)

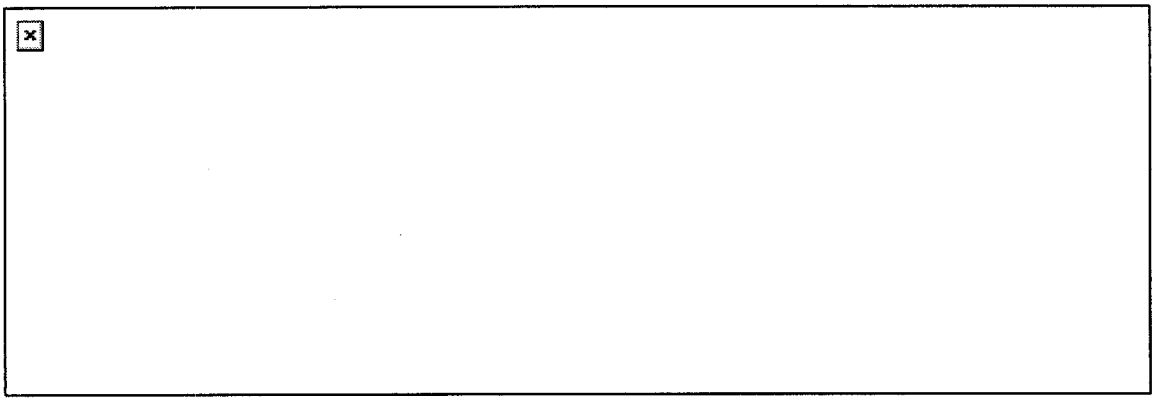

Figure 5: (left) Geostorm Sailcraft Peak X and Y Body Rate History (assuming X, then Y axis torque sequence) for entire L1-to-sub-L1 transfer, based on commanded cone and clock angles; (right) "zoom" of one region of the peak body rates

The peak control torque level predicted for the given control history and the given sail configuration is around 7×10^{-5} N-m. This torque level could be satisfied, for example, with a set of vanes with reflective area not smaller than 0.22 m^2, at the end a 70.71 m boom extending from the sail center (implied by a 100-m square sail side), assuming a near-Earth local solar radiation pressure of about 4.5×10^{-6} N/m^2.

Conclusions and Future Work

The results discussed in this paper are based on an initial implementation in a sailcraft trajectory propagator of targeted-torque rotation modeling, to achieve a six-degree-of-freedom simulation of sailcraft motion. Further testing of this 6DOF-modified propagator is presently underway. Present plans are to test the propagator with a different mission profile than Geostorm, perhaps an Earth-orbiting sailcraft trajectory, in order to more fully evaluate the strengths and limitations of the approach. Of particular interest is testing this formulation with a spinning sailcraft. Finally, the 6DOF-modified trajectory propagator is being incorporated into a trajectory optimizer for NASA's S5 project. This new trajectory optimizer will take advantage of the six-degree-of-freedom formulation, in particular the analytic formulation, in order to torque constraints, in addition to attitude and body rate constraints that are typical of the current state of the art in sailcraft optimization.

Acknowledgements

The work reported here was performed at the California Institute of Technology Jet Propulsion Laboratory under NASA contract TTA 800-53-01. Also, the author thanks Dr. Chen-Wan Yen of JPL for providing the Geostorm optimal trajectory and control profile used in these analyses.

References

1. L. Rios-Reyes and D. J. Scheeres, "Generalized Models for Solar Sails." Paper AAS 04-286 of the 14th AAS/AIAA Spaceflight Mechanics Meeting, Maui, HI, Feb. 2004.

2. C. McInnes, *Solar Sailing – Technology, Dynamics, and Mission Applications*. Springer Publications, 1999.

3. C. G. Sauer, Jr., "Optimum Solar-Sail Interplanetary Trajectories," Paper No. 76-0792 of the AIAA/AAS Astrodynamics Conference, San Diego, CA, Aug. 1976.

4. G. Colasurdo and L. Casalino, "Optimal Control Law for Interplanetary Trajectories with Solar Sail." Paper AAS 01-469 of the AAS/AIAA Astrodynamics Specialists Conference, Quebec City, Quebec, Canada, Aug. 2001.

5. C. G. Sauer, Jr., "The L1-Diamond Affair." Paper AAS 04-278 of the 14th AAS/AIAA Spaceflight Mechanics Meeting, Maui, HI, Feb. 2004.

6. V. Bond and M. C. Allman, *Modern Astrodynamics*. Princeton Press, 1996.

7. W. H. Press, B. P. Flannery, S. A. Teukolsky, W. T. Vetterling. *Numerical Recipes: The Art of Scientific Computing*. Cambridge University Press, 1990.

8. J. Ellis, M. Lisano, P. Wolff, J. Evans, J. Bladt, D. Scheeres, L. Rios-Reyes, and D. Lawrence, "A Solar Sail Integrated Simulation Toolkit." Paper AAS 04-283 of the 14th AAS/AIAA Spaceflight Mechanics Meeting, Maui, HI, Feb. 2004.

9. C. W. Yen, "Solar Sail Geostorm Warning Mission Design." Paper AAS 04-107 of the 14th AAS/AIAA Spaceflight Mechanics Meeting, Maui, HI, Feb. 2004.